JOURNAL OF VIROLOGY, July 2005, p. 8687–8697 Vol. 79, No. 14
0022-538X/05/$08.00+0 doi:10.1128/JVI.79.14.8687–8697.2005
Copyright © 2005, American Society for Microbiology. All Rights Reserved.

Stimulation of Hepatitis C Virus (HCV) Nonstructural Protein 3 (NS3) Helicase Activity by the NS3 Protease Domain and by HCV RNA-Dependent RNA Polymerase

Chen Zhang,[1] Zhaohui Cai,[1] Young-Chan Kim,[2] Ranjith Kumar,[2] Fenghua Yuan,[1] Pei-Yong Shi,[3] Cheng Kao,[2] and Guangxiang Luo[1]*

Department of Microbiology, Immunology and Molecular Genetics, University of Kentucky College of Medicine, Lexington, Kentucky 40536[1]; Department of Biochemistry and Biophysics, Texas A&M University, College Station, Texas 77843-2128[2]; and Wadsworth Center, New York State Department of Health, Albany, New York 12201[3]

Received 17 January 2005/Accepted 22 March 2005

Hepatitis C virus (HCV) nonstructural protein 3 (NS3) possesses multiple enzyme activities. The N-terminal one-third of NS3 primarily functions as a serine protease, while the remaining two-thirds of NS3 serve as a helicase and nucleoside triphosphatase. Whether the multiple enzyme activities of NS3 are functionally interdependent and/or modulated by other viral NS proteins remains unclear. We performed biochemical studies to examine the functional interdependence of the NS3 protease and helicase domains and the modulation of NS3 helicase by NS5B, an RNA-dependent RNA polymerase (RdRp). We found that the NS3 protease domain of the full-length NS3 (NS3FL) enhances the NS3 helicase activity. Additionally, HCV RdRp stimulates the NS3FL helicase activity by more than sevenfold. However, the helicase activity of the NS3 helicase domain was unaffected by HCV RdRp. Glutathione *S*-transferase pull-down as well as fluorescence anisotropy results revealed that the NS3 protease domain is required for specific NS3 and NS5B interaction. These findings suggest that HCV RdRp regulates the functions of NS3 during HCV replication. In contrast, NS3FL does not increase NS5B RdRp activity in vitro, which is contrary to a previously published report that the HCV NS3 enhances NS5B RdRp activity.

Hepatitis C virus (HCV) infection causes liver diseases such as chronic hepatitis, cirrhosis, and hepatocellular carcinoma. It infects approximately 170 million people worldwide, and the majority of HCV-exposed individuals become persistently infected (51, 57). HCV belongs to the *Hepacivirus* genus of the *Flaviviridae* family and is divided into six major genotypes and numerous subtypes based on genome sequence heterogeneity (13, 48). The viral genome is a single-stranded positive-sense RNA that encodes a single open reading frame (7, 8). Upon translation, the polyprotein is processed by both cellular and viral proteases into individual structural and nonstructural (NS) proteins (47). The structural proteins (E1, E2, C, and probably p7) are proteolytically cleaved from the N-terminal portion of the viral polyprotein by cellular signal peptidases (17, 31, 52), while the NS proteins (NS2, NS3, NS4A, NS4B, NS5A, and NS5B) are produced by the polyprotein processing at the NS2–NS3 junction by the NS2-3 metalloprotease and at the downstream sites of NS3 by the NS3 serine protease (1, 10, 21, 32, 33).

HCV structural proteins are required for virus entry, assembly, and egression, while the NS proteins play many important roles in viral polyprotein processing, RNA replication, and pathogenesis (2, 3, 39, 49). A significant advance in the understanding of HCV replication was the establishment of subgenomic replicons of HCV, which can replicate in the cultured cells (5, 34). These studies revealed that NS3, NS4A, NS4B, NS5A, and NS5B proteins are sufficient for RNA replication. Mutational analysis of replicable HCV RNAs further implied that the NS3 to -5B proteins likely represent the core set of viral proteins necessary for HCV RNA replication in vivo (12, 29, 36). These proteins colocalize with each other and with the replicating HCV RNA predominantly in the perinuclear membrane regions (12, 54). Also, subcellular fractionation studies demonstrated that each of the NS3 to -5B proteins was localized in the same membrane fraction (12, 54). These findings suggest that the NS3 to -5B proteins form a membrane-bound multiprotein complex where HCV RNA replicates. The interaction of these proteins and the effects of those interactions on viral RNA replication remain poorly understood. It is clear, however, that NS3 and NS5B are essential for HCV replication in vivo (29).

NS3 is a multifunctional protein possessing protease, helicase, and nucleoside triphosphatase (NTPase) activities located in two functionally distinct domains (1, 10, 16, 21, 22, 25, 26, 30, 56). The N-terminal one-third of NS3 primarily serves as a serine protease that associates with NS4A to proteolytically process the viral polyprotein at the junctions between NS3/4A, 4A/4B, 4B/5A, and 5A/5B (10). This region is also required for the NS2-3 metalloprotease responsible for cleavage at the NS2–NS3 junction (16, 21, 59). The C-terminal two-thirds of NS3 have helicase and NTPase activities (25, 26). A number of biochemical studies demonstrated that the protease and helicase domains of NS3 are active when expressed separately in vitro (25, 26, 38, 55). However, there is no evidence to suggest that the protease and helicase domains of

* Corresponding author. Mailing address: Department of Microbiology, Immunology and Molecular Genetics, University of Kentucky College of Medicine, 800 Rose Street, Lexington, KY 40536. Phone: (859) 257-5577. Fax: (859) 257-8994. E-mail: gluo0@uky.edu.

Downloaded from http://jvi.asm.org/ on September 12, 2018 by guest

NS3 are proteolytically cleaved during HCV replication in the cell. There is circumstantial evidence suggesting that the NS3 protease domain might modulate its helicase activity in vitro (22, 23, 40). This observation, however, remains to be confirmed.

NS5B is the viral RNA-dependent RNA polymerase (RdRp) responsible for catalyzing RNA polymerization during HCV replication (4). Replication of HCV RNA takes place in the membrane-bound replication complex (11, 12, 41, 54). Both NS3 and NS5B are assumed to function together during HCV RNA replication. One model is that the NS3 helicase could unwind RNA secondary structures and/or a double-stranded RNA (dsRNA) intermediate before RNA synthesis by NS5B (43). NS3 was reported to interact with NS5B and with NS4A in the cell (24). A recent report by Piccininni et al. suggested that the HCV NS3 protein interacts with NS4B and NS5B in far Western blot assays. Furthermore, they observed that NS3 could stimulate NS5B RdRp activity (44). Whether the HCV RdRp modulates NS3 helicase activity has not been experimentally examined.

In this study, we expressed and purified a full-length NS3 (NS3FL), a truncated NS3 helicase domain (NS3H), and NS5B of HCV genotype 1b. The enzyme activities of these recombinant proteins were directly compared in vitro. We show that the NS3FL was about fivefold more active than NS3H in helicase but not NTPase activity, suggesting that the NS3 protease domain contributes to helicase activity. Additionally, HCV RdRp (NS5B) was found to stimulate the NS3 helicase but not NTPase activity. In contrast, NS5B failed to stimulate the helicase of NS3H, suggesting that the NS3 protease is required for helicase stimulation by NS5B. Glutathione *S*-transferase (GST) pull-down experiments and fluorescence spectroscopy analysis were performed to determine whether the NS3 protease domain mediates a protein-protein interaction between NS3 and NS5B. Interestingly, NS5B was found to specifically interact with NS3FL but not NS3H. These findings suggest a possible coordination between the HCV RdRp activity and helicase activity through the NS3 protease domain. In contrast, the NS3-NS5B interaction did not significantly affect NS5B RdRp activity in vitro on HCV-specific or nonviral RNA templates.

MATERIALS AND METHODS

DNA construction. Both cDNAs encoding NS3FL and the C-terminal 450 amino acids of the NS3 helicase domain (NS3H) of HCV genotype 1b were amplified by PCR using pBR322/I377-NS3-3′/S1179I (37) as a template and different sets of synthetic oligonucleotide primers. 1b-His-NS3 (5′-CGCGCCATGGCACACCACCACCACCACCACGCGCCTATTACGGCCTACTC-3′) and 1b-NS3-EcoRI (5′-GGAATTCTACGTGACGACCTCCAGGTCAG-3′) were used for PCR amplification of NS3FL cDNA. The PCR DNA was cut by restriction enzymes NcoI and EcoRI and cloned into pET21d vector (Novagen) that was also digested with NcoI and EcoRI. The NS3H cDNA was amplified by PCR using NS3H-BspHI (5′-GCGCAAGCTTCATGAGGTCCCCGGTCTTCACGGAC-3′) and NS3-His (5′-CGCGAAGCTTCAGTGGTGGTGGTGGTGGTGCGTGACGACCTCCAGGTCAG-3′) as primers. PCR DNA was digested with BspHI (NcoI compatible) and HindIII and inserted into the vector pET-21d similarly cut by the same enzymes. The resulting DNA constructs were designated pET-21d-NS3FL and pET-21d-NS3H, respectively. An amino acid mutation from cysteine to histidine at residue 292 (C292H) was introduced by two-step PCR using two sets of primers. The 5′-end portion of the DNA was amplified using primers NS3-NcoI (5′-CATGCCATGGCGCCTATTACGGCCTAC-3′) and C292H/3 (5′-GTGGTGCTCATCACATATTATGATGC-3′), while the 3′ portion was amplified with C292H/5 (5′-TAATATGTGATGAGCACCACTCAACTGACTC-3′) and NS3-His as primers and pET-21d-NS3FL as a template. For the second-round PCR, both 5′ and 3′ PCR DNAs were used as templates and NS3-NcoI and NS3-His were used as primers. The PCR DNA was digested with NcoI and HindIII and cloned into pET21d vector between NcoI and HindIII sites, resulting in pET21d/NS3FL-C292H. The NS5B cDNA was also amplified by PCR using NS5B-BspHI (5′-CGGGATCCTCATGAGCATGTCCTACACATGGACAGGC-3′) and NS5BΔ21-XhoI (5′-CGCGCTCGAGTCAGTGGTGGTGGTGGTGGCGGGGTCGGGCACGAGACAGGC-3′) as primers and pBR322/I377-NS3-3′/S1179I as a template. PCR DNA was digested with BspHI (compatible with NcoI site) and XhoI and inserted into pET21d vector between the NcoI and XhoI sites. A His_6 tag was added to either the N or C termini of NS3 and NS5B proteins to facilitate protein purification.

To express a GST-NS5B fusion protein, the cDNA of NS5B of genotype 1b was amplified by PCR using pBR322/I377-NS3-3′/S1179I as a template and NS5B-BspHI and NS5BΔ21-XhoI as primers. The NS5B PCR product was digested by BamHI and XhoI and inserted into a pGEX-4T-1 vector (Amersham Pharmacia Biotech), which was similarly digested with BamHI and XhoI, resulting in a construct designated pGEX-4T/NS5B.

The West Nile virus (WNV) RdRp (amino acids 266 to 905) cDNA was PCR amplified from an infectious cDNA clone of a New York strain of WNV (53) and cloned into the expression vector pET-28a (Novagen) between the restriction enzyme sites NdeI and XhoI, resulting in a construct designated pET-28a-WNV-RdRp. The WNV RdRp expressed from pET-28a-WN-RdRp contained a His_6 tag at the N terminus.

Protein expression and purification. NS3FL, NS3H, HCV NS5BΔ21, and WNV RdRp were expressed in *Escherichia coli* strain BL21 (Novagen). The cultures were grown in LB medium at 37°C until the optical density at 600 nm (OD_{600}) reached 1.0 and induced by addition of isopropyl-β-D-thiogalactopyranoside (IPTG) to 1 mM. After an additional incubation at 18°C for 20 h, cells were harvested by centrifugation at 6,000 × *g* for 10 min and resuspended in a lysis buffer containing 50 mM Na_3PO_4, pH 8.0, 300 mM NaCl, 5 mM 2-mercaptoethanol, 10% glycerol, 0.5% Igepal CA630, and a protease inhibitor cocktail consisting of 1 mM phenylmethylsulfonyl fluoride, 0.5 μg/ml leupeptin, pepstatin A, and 2 mM benzamidine. Cells were lysed by freezing and thawing, followed by sonication. Cell debris was removed by centrifugation at 12,000 × *g* for 30 min. The supernatant was further clarified by passing though a 0.45-μm filter (Corning) and then loaded onto a HiTrap chelating column charged with $NiSO_4$ (Amersham Pharmacia Biotech). The bound protein was eluted with an imidazole solution in a 100-to-500 mM linear gradient. Selected fractions through Ni^{2+} column chromatography were analyzed on a 10% sodium dodecyl sulfate (SDS)-polyacrylamide gel. Protein concentrations were determined by spectrophotometry using the calculated extinction coefficients for each protein. For expression of a GST-NS5B fusion protein, *E. coli* strain BL21pLysS(DE3) transformed with pGEX-4T/NS5B was grown at 37°C in LB medium containing 100 μg/ml of ampicillin to an OD_{600} of 0.6. The protein expression was induced by addition of 0.4 mM IPTG at 25°C for 8 h. Bacteria were harvested, pelleted down, and resuspended in phosphate-buffered saline (PBS) buffer, containing 1% Triton X-100, and protease inhibitor cocktail described above. Lysates clarified as described above were loaded onto a GSTrap HP column (Amersham Pharmacia Biotech). The column was washed with PBS buffer. The bound GST-NS5B fusion protein was eluted with an elution buffer (50 mM Tris-HCl and 10 mM reduced glutathione; pH 8.0). The pooled GST fusion protein fractions were concentrated by polyethylene glycol 8000 and then loaded onto a fast performance liquid chromatography (FPLC) Superdex-200 gel filtration column that was equilibrated in FPLC buffer (50 mM Tris-HCl, pH 7.5, 10% glycerol, and 5% β-mercaptoethanol containing 150 mM KCl). The GST fusion protein was confirmed by Western blot analysis. The purity of the isolated proteins was examined by electrophoresis on a 10% SDS-polyacrylamide gel electrophoresis (SDS-PAGE) gel and stained with Coomassie blue. The control GST protein was also expressed and purified using the same protocol. The purified proteins were divided into aliquots and stored at −80°C.

The WNV RdRp was expressed in *E. coli* BL21 in LB medium at 30°C to an OD_{600} of about 0.8 and induced by addition of 1 mM IPTG at 30°C for 4 h. Otherwise, the purification scheme was the same as for HCV NS5B.

Western blot analysis. Purified NS3H, NS3FL, and NS5BΔ21 proteins were resolved by electrophoresis in a 12% SDS-PAGE gel and then transferred onto a nitrocellulose membrane. The HCV proteins were determined by Western blot analysis using monoclonal antibodies against NS3 and NS5B proteins. Proteins were visualized by using a chemiluminescence kit (Roche) with horseradish peroxidase-conjugated goat anti-mouse antibodies (Pierce) as secondary antibodies.

Preparation of NS3 helicase substrate. A short dsDNA was formed by hybridization of two synthetic oligonucleotides, a 30-nucleotide (nt) releasing strand

Downloaded from http://jvi.asm.org/ on September 12, 2018 by guest

(5′-TGGTACTCCTCACACCTGGGCGGCGGTTAA-3′) and a 54-nt DNA (5′-GACTACGTACTGTTAACCGCCGCCCAGGTGTGAGGAGTACCAG GCCAGATCTGC-3′). The 30 nt were labeled with ^{32}P at the 5′ end by use of [γ-^{32}P]ATP (MP Biomedicals) and T4 polynucleotide kinase (New England Biolabs) at 37°C for 1 h. Unincorporated [γ-^{32}P]ATP was removed by passing through a Sephadex G-50 column (Roche). The radiolabeled 30-nt DNA was used to anneal to an equal molar amount of longer-strand DNA (54 nt) to form a partial dsDNA. NS3 helicase substrate has a 12-nt overhang at both the 5′ and 3′ ends of the longer-strand DNA.

Helicase assay. The NS3 helicase was assayed in a 10-μl reaction mixture containing 20 mM HEPES, pH 7.5, 2 mM dithiothreitol, 100 μg/ml bovine serum albumin, 3 mM $MgCl_2$, various amounts of enzyme and substrate as indicated, and 0.5 pmol of a 30-nt capture oligonucleotide (5′-TTAACCGCCGCCCAGG TGTGAGGAGTACCA-3′). The reaction was initiated by addition of 5 mM ATP and incubated at 37°C for 30 min and then stopped by addition of a glycerol loading buffer containing 20 mM EDTA and 0.5% SDS. The products were analyzed in a 12% native polyacrylamide gel and quantitated with a PhosphorImager (Molecular Dynamics). The unwound products were calculated as the percentage of the total DNA substrate. A synthetic NS4A core peptide (KK-G SVVIVGRIILSGRPAIVP-KK) was used for its effect on the NS3FL helicase activity. To determine the effects of NS5B on NS3 helicase activity, increasing amounts of NS5B were added into the helicase reaction mixture. As controls, increasing amounts of WNV RdRp or HCV NS5BΔ21 itself were incubated with a partially duplex DNA substrate under the same reaction conditions as above.

NTPase assay. The protocol of Cui et al. was used to assay NTPase activity (9). Briefly, the 10-μl reaction mixture contained 20 mM HEPES, 3 mM $MgCl_2$, 2 mM dithiothreitol, 100 μg/ml bovine serum albumin, 0.5 mM cold ATP spiked with 1 μCi [γ-^{32}P]ATP (4,500 Ci/mmol; MP Biomedicals), and NS3FL or NS3H at the indicated concentrations. The reaction mixture was incubated at 37°C for 30 min and then stopped by the addition of EDTA to 50 mM. One-tenth of the reaction mixture was spotted onto a thin-layer chromatography plate coated with polyethyleneimine cellulose (J.T. Baker). The radioactive phosphate hydrolyzed from [γ-^{32}P]ATP was separated by chromatography using 0.375 M potassium phosphate (pH 3.5) as a running buffer. The hydrolyzed phosphate was quantified with a PhosphorImager (Molecular Dynamics).

GST pull-down assay. GST protein (2 μg) or a GST-NS5B fusion protein (2 μg) was incubated with 20 μl of a 50% slurry of glutathione-agarose gel at 4°C for 2 h with rotation. After washing with PBST buffer (phosphate-buffered saline containing 1% Triton X-100), GST-bound resins were incubated with 2 μg of His-tagged NS3 protein in 300 μl of PBS buffer containing 0.5% Igepal CA630 at 4°C for 2 h and then washed with NETN 300 buffer (20 mM Tris-HCl, pH 7.4, 0.1 mM EDTA, and 300 mM NaCl). Proteins bound to the glutathione-agarose gel (Pierce) were resuspended in a loading buffer, denatured, and loaded into a 10% SDS-PAGE gel. Proteins were subsequently transferred onto a membrane, followed by Western blot analysis using an anti-NS3H monoclonal antibody.

Analysis of NS3FL-NS5B interaction using fluorescence spectroscopy. Fluorescence measurements were made at room temperature (22 to 23°C) with a Perkin-Elmer luminescence spectrometer LS55 and cuvettes with an optical path length of 0.4 cm. Equilibrium anisotropy measurements were performed with a version of the HCV NS5BΔ21 protein which was engineered to have a tetracysteine motif capable of binding to the FlAsH dye (Y. C. Kim, unpublished data). When dialyzed with the FlAsH dye, approximately 15% of the protein will incorporate a dye molecule. After removal of the free dye, NS5BΔ21 at 0.2 μM was titrated with increasing concentrations of NS3FL in buffer A (50 mM HEPES, pH 7.5, 50 mM NaCl, 5 mM $MgCl_2$, and 0.002% Tween 20). Measurements were taken with an integration time of 1 second and a slit width of 5 nm of both excitation (500 nm) and emission (530 nm). Anisotropy values were recorded after 20 s after each addition of NS3FL to allow the sample to reach equilibrium. Anisotropy measurements were repeated 10 times for each sample, and the resulting values were averaged.

Binding data were analyzed by nonlinear least square fitting using KaleidaGraph software (Synergy Software, Reading, PA). The Hill equation was used to determine the K_d as follows: $\Delta A = B_{max}\, x^n/(x^n + K_d{}^n)$ (Hill equation). In this equation, ΔA is the value of anisotropy change by the ligand binding, B_{max} is the value of maximum anisotropy change, x is the total concentration of the input NS3FL, and the exponential term (n) is the Hill coefficient, which can be used to estimate the extent cooperative binding.

RdRp activity assays. Standard RdRp assays consisted of 0.125 μM of template RNA with 0.08 μM of NS5B in a 20-μl reaction mixture containing 20 mM sodium glutamate (pH 8.2), 4 mM $MgCl_2$, 12.5 mM dithiothreitol, 0.5% (vol/vol) Triton X-100. Reactions with LE21 as template had 200 μM GTP, 100 μM ATP and UTP, and 250 nM [α-^{32}P]CTP (Amersham Inc.). Where indicated, NS3FL and NS3H were at 1× (1:1) and 2× (1:2) that of NS5B. Assays were performed with both NS5BΔ21 and full-length NS5B (NS5BFL). The assay using template H121 was performed only with NS5BΔ21 at 1:1 and 1:2 molar ratios of NS5B to NS3. One part of the reaction was performed with 200 μM GTP, 100 μM ATP and UTP, and 500 nM [α-^{32}P]CTP, and the other was with 200 μM GTP, 100 μM ATP and CTP, and 500 nM [α-^{32}P]UTP. In all cases, the reaction mixture was adjusted for the final buffer content. RNA synthesis reaction mixtures were incubated at 25°C for 60 min and stopped by phenol-chloroform extraction followed by ethanol precipitation in the presence of 5 μg of glycogen and 0.5 M ammonium acetate. Products were separated by electrophoresis on denaturing (7.5 M urea) polyacrylamide gels. Gels were wrapped in plastic and exposed to film at −80°C.

RESULTS

Protein expression and purification. The goal of this study was to analyze the possible contributions of both the NS3 helicase and protease domains to known activities and for possible interactions between NS3 and NS5B. All of the proteins, NS3FL, NS3H, NS5BΔ21, NS5BFL, and the WNV RdRp, were expressed in *E. coli* and purified through Ni^{2+} column chromatography to greater than 95% purity in Coomassie blue-stained denaturing protein gels (Fig. 1A and data not shown). Additionally, the identities of the NS3 and NS5B proteins were confirmed by Western blot analysis using NS3- and NS5B-specific antibodies (Fig. 1B).

Comparison of enzyme activities of purified recombinant NS3FL and NS3H. It has been previously demonstrated that HCV NS3 is able to unwind partially duplex nucleic acids (RNA-RNA, RNA-DNA, or DNA-DNA) without exhibiting substrate specificity in vitro (19, 20, 30). Also, NS3 helicase requires a 3′-end single-stranded overhang in order for initiation of duplex unwinding in the 3′-to-5′ direction (19). Therefore, a partial dsDNA substrate was prepared by annealing a 30-nt synthetic DNA to a 54-nt DNA, resulting in a 12-nt single-stranded DNA overhang at both the 5′ and 3′ ends (Fig. 2A). A 30-nt capture oligonucleotide, which is fully complementary to the radiolabeled short DNA strand, was added in fivefold excess to the helicase reaction mixture in order to stop the reannealing of the released strand back to the longer DNA strand. The newly formed dsDNA between the capture DNA and the released strand was fully complementary and should not serve as a substrate for NS3 helicase (Fig. 2A). This assay was initially validated by NS3FL. As shown in Fig. 2B, NS3FL helicase activity efficiently unwound the partially duplexed DNA in a dose-dependent manner (Fig. 2B and C). The substrate unwinding was linearly correlated with increasing amounts of enzyme up to 0.4 pmol and reached a maximum at 0.8 pmol protein (Fig. 2C). In contrast, NS3FL/C292H, which contains a cysteine-to-histidine mutation at amino acid 292 in the conserved helicase DCEH motif (30), failed to unwind dsDNA (Fig. 2B and C). These results demonstrate that the substrate unwinding by NS3FL was the activity of the HCV NS3 protein. In addition, we examined the protease activity of purified NS3FL using an in vitro-translated NS5A-NS5B protein as substrate. NS3FL was able to efficiently cleave an NS5A-NS5B precursor into NS5A and NS5B proteins (data not shown). Taken together, these findings demonstrate that purified NS3FL contains both functional protease and helicase activities.

Circumstantial evidence derived from previous studies suggests that the protease and helicase/NTPase domains of the NS3 are functionally interdependent (23, 40, 42). To further

Downloaded from http://jvi.asm.org/ on September 12, 2018 by guest

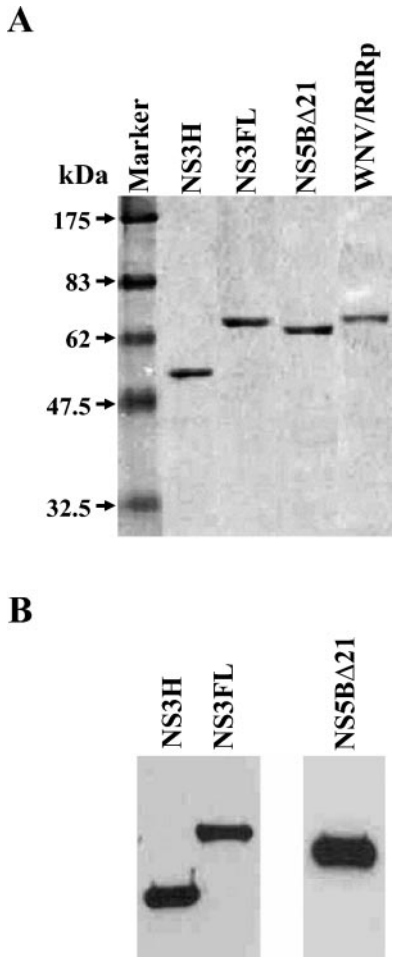

FIG. 1. (A) Electrophoresis analysis of purified recombinant NS3 and NS5B proteins. Protein expression and purification are described in Materials and Methods. Two hundred nanograms of each protein was loaded onto a 12% polyacrylamide–SDS gel. Protein bands were visualized by Coomassie blue staining. The name of the protein is shown on the top, and the sizes of protein molecular mass markers are indicated on the left. (B) Confirmation of NS3 and NS5B proteins by Western blot analysis. NS3H, NS3FL, and NS5B were separated as for panel A and then transferred onto a nitrocellulose membrane. Monoclonal antibodies specific to NS3 and NS5B were used for Western blot analysis.

determine the effect of the protease domain on the enzyme activities of the helicase domain, we directly compared the helicase and NTPase activities between NS3FL and NS3H. As shown in Fig. 3, NS3FL unwound the substrate more efficiently than NS3H. The substrate unwinding was proportional to increasing amounts of NS3FL up to 0.8 pmol protein, at which it reached a maximum unwinding at 85% of total substrate. However, NS3H unwound the duplex DNA substrate less efficiently and did not reach the plateau until at least 3.2 pmol of protein was used (Fig. 3A). Since fivefold more NS3H than NS3FL was required to achieve a similar substrate unwinding, the presence of the NS3 protease domain significantly enhances the NS3 helicase activity. This finding was confirmed by using a previously described RNA substrate (14). Similar to unwinding of dsDNA substrate, NS3FL unwound the partially duplex RNA more efficiently than NS3H (data not shown). These results are consistent with previous findings that HCV NS3 helicase does not discriminate DNA and RNA substrates in vitro (19, 20, 30). Additionally, a synthetic NS4A core peptide (KK-GSVV IVGRIILSGRPAIVP-KK) (58) was found to stimulate the NS3FL helicase by up to fourfold at a 100 μM concentration (data not shown). In contrast, there was no significant difference in their NTPase activities when NS3FL and NS3H were compared in parallel (Fig. 3B). We also examined the NTPase activities of NS3FL and NS3H in the presence of dsDNA substrate and did not observe any significant difference in NTPase activity (data not shown). These findings indicate that the enhancement of the NS3 helicase by the protease domain was not due to NTPase activation and that both proteins were properly folded for NTPase activity. This is consistent with a previous observation that the NS3 NTPase is uncoupled with its helicase translocation (43). Thus, the NS3 protease domain specifically up-regulates the NS3 helicase activity.

Specific stimulation of NS3 helicase by HCV RdRp. Both NS3 helicase and NS5B RdRp are required for HCV RNA replication (29). It was previously reported that NS3 colocalized with NS5B in the cell (24). Whether the NS3 helicase activity is modulated by direct interaction between NS5B and NS3 has not been experimentally examined. Therefore, we determined whether NS5B affects the NS3 helicase activity in vitro. We first determined whether the unwinding efficiency changed over time. When a 5:1 ratio of the enzyme and substrate was used, the NS3FL helicase efficiently unwound the DNA substrate with a maximum unwinding efficiency reached within 30 min. More than 50% of substrate was actually unwound within 5 min (Fig. 4). When the enzyme and substrate ratio was reduced to 1:1 (0.1 pmol enzyme and substrate), the substrate unwinding efficiency was much less, with release of only about 10% of substrate even after 60-minute incubation (Fig. 4). A suboptimal substrate unwinding efficiency would be more likely to reveal whether NS5B stimulates the NS3FL helicase activity. Accordingly, the helicase activity of NS3FL was examined in the presence of increasing amounts of NS5BΔ21 protein. As shown in Fig. 5, the efficiency of substrate unwinding was proportionally correlated with increasing concentrations of NS5BΔ21. Based on the substrate unwinding efficiency, it was estimated that NS5BΔ21 stimulated the NS3 helicase by seven- to eightfold (Fig. 5 and 6). As a control, NS5B itself did not display any helicase activity (Fig. 5). To rule out the possibility that NS5B might stimulate the NTPase activity, since the helicase is coupled with ATP hydrolysis, we examined the effect of NS5B on the NS3FL NTPase activity. Results from this experiment did not show any effect of NS5B on the NS3FL NTPase (data not shown). To further determine the specificity of the NS3 helicase stimulation by HCV RdRp, the RdRp from West Nile virus, also a flavivirus, was used in the NS3FL helicase assay and found to not exhibit any stimulatory activity at all on the HCV NS3 helicase. Taken together, these findings clearly demonstrate that HCV RdRp specifically stimulated the NS3FL helicase but not NTPase activity in vitro, suggesting a cooperative up-regulation of the NS3 helicase by RdRp during HCV RNA replication.

Requirement of the NS3 protease domain for helicase stimulation by NS5B. To determine whether the NS3FL helicase stimulation by RdRp requires the NS3 protease domain, NS3H was used in the helicase assay. Since the NS3H was about

Downloaded from http://jvi.asm.org/ on September 12, 2018 by guest

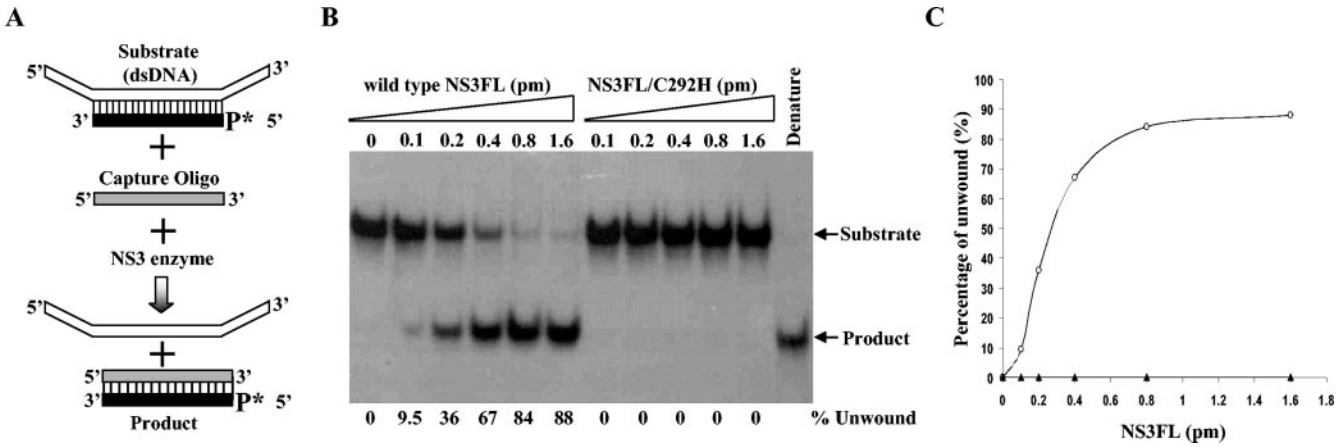

FIG. 2. (A) Schematic of the helicase assay. A synthetic 30-nt oligonucleotide was annealed to a 54-nt DNA to form a partially duplex DNA substrate. Upon duplex unwinding by NS3 helicase, the 5′-end ^{32}P-radiolabeled release strand (indicated by P* at the 5′ end) is trapped by a complementary capture oligonucleotide. (B) Titration of the NS3FL helicase. A 0.1-pmol aliquot of dsDNA substrate was incubated with increasing amounts of NS3FL or an inactive helicase mutant, NS3FL/C292H, at 37°C for 30 min. The unwound substrate products were analyzed in a native 12% polyacrylamide gel. The percentage of substrate unwound, indicated at the bottom, was determined by from the quantitative data derived from phosphorimager results. Amounts of NS3FL used are indicated on the top. (C) Correlation of NS3FL helicase activity with enzyme concentrations. The quantitative data are derived from panel B.

fivefold lower in helicase activity than NS3FL, an approximately equivalent substrate unwinding activity of NS3H to NS3FL was used in the helicase assay. Contrary to NS3FL, the NS3H helicase activity was not significantly affected by the addition of increasing amounts of NS5BΔ21 (Fig. 6). These results demonstrate that the NS3 protease domain was required for helicase stimulation by NS5B. This finding also suggests that the NS3 protease domain might mediate a specific protein-protein interaction between NS3FL and NS5B.

NS3-NS5B interaction revealed by GST pull-down. To determine a protein-protein interaction between NS3 and NS5B, a GST pull-down experiment was performed. NB5B bound to glutathione-agarose was incubated with either NS3FL or NS3H protein. GST protein alone was used as a control in this experiment. Coprecipitated proteins were detected by Western blot analysis using a monoclonal antibody against the NS3 helicase domain. As shown in Fig. 7, NS5B specifically pulled down the NS3FL but not NS3H (Fig. 7), suggesting that the protease domain was required for NS3 and NS5B interaction. GST did not pull down any NS3 protein, demonstrating that the NS3 protease mediated a specific NS3-NS5B interaction.

Determination of NS5B and NS3FL interaction by fluorescence spectroscopy. To more quantitatively analyze the interaction between NS5B and NS3FL, we used a recombinant NS5BΔ21 molecule that has been engineered to bind the FlAsH dye (18). This protein is fully capable of de novo initiating RNA synthesis and does not appear to be significantly affected in any of the known activities (Y. C. Kim, unpublished

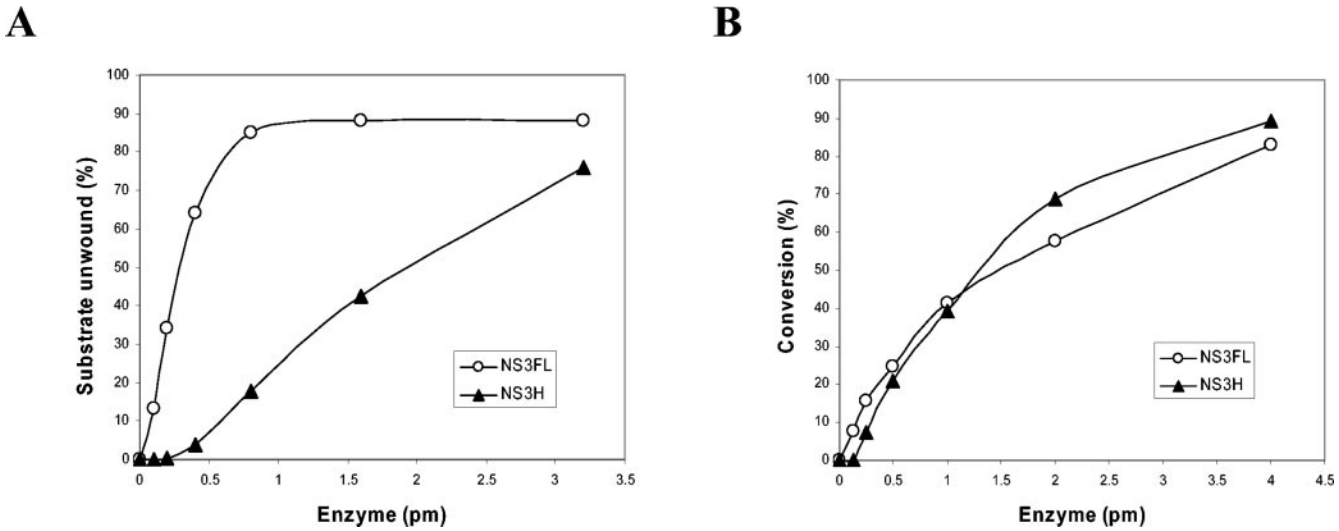

FIG. 3. (A) Comparison of helicase activities of NS3FL and NS3H. The helicase assay was the same as that in Fig. 2. (B) Comparison of the NTPase activities of NS3FL and NS3H. The NTPase activity is expressed as the percentage of radioactive phosphate converted from [γ-^{32}P]ATP. The enzyme concentrations (*x* axis) are plotted against the percentage of conversion of phosphate from ATP (*y* axis). ○, NS3FL; ▲, NS3H.

Downloaded from http://jvi.asm.org/ on September 12, 2018 by guest

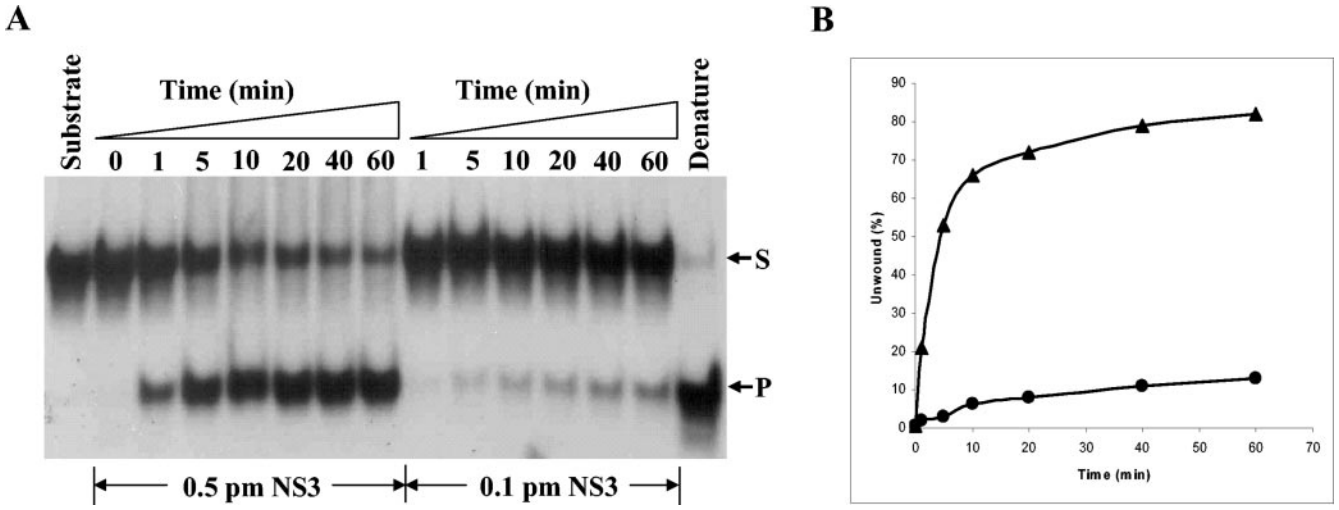

FIG. 4. (A) Time course of NS3FL helicase activity. A 0.1-pmol aliquot of dsDNA substrate was incubated with either 0.1 pmol or 0.5 pmol NS3FL enzyme (as indicated at the bottom) at 37°C. At different time points (indicated on the top), the reactions were stopped by addition of a loading buffer containing 20 mM EDTA and 0.5% SDS. The unwound products were analyzed in a 12% native polyacrylamide gel, visualized by autoradiograph, and quantified by use of a phosphorimager. (B) Relation of NS3FL helicase activity to incubation time. The quantitative data from panel A were used to plot the incubation time (*x* axis, in min) against the percentage of unwound substrate (*y* axis). ●, 0.1 pmol NS3FL; ▲, 0.5 pmol NS3FL.

data). However, having a dye-labeled version of NS5BΔ21 allowed us to examine the properties of the protein even in the presence of other molecules that could otherwise affect the spectroscopic properties of the solution. In the presence of increasing NS3FL, we observed a significant change in the anisotropy of NS5BΔ21 that started to saturate when NS3FL protein reached about 5 μM (Fig. 8). The binding isotherm was used to derive the affinity of the NS5B-NS3FL interaction, with a K_d of approximately 2 μM. In contrast, the K_d for interaction between NS5BΔ21 and NS3H was higher than 50 μM (Fig. 8). Therefore, these results from fluorescence anisotropy are in agreement with those from the GST pull-down assays (Fig. 7), demonstrating that the NS3 protease domain is required for a tighter interaction with NS5B.

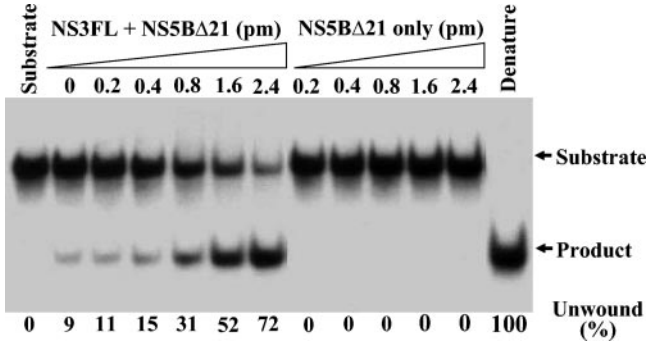

FIG. 5. Stimulation of NS3FL helicase activity by HCV RdRp. A partially duplex DNA substrate was incubated with 0.1 pmol NS3FL and increasing amounts of NS5BΔ21 at 37°C for 30 min (left panel). As controls, the helicase substrate was incubated with increasing amounts of NS5B in the absence of NS3FL (right panel). The unwound substrate products were resolved in a 12% native polyacrylamide gel, visualized by autoradiograph, and quantified with a phosphorimager. The percentage of unwound substrate is shown at the bottom, and the amounts of NS5B are indicated on the top.

Effect of NS3 on RdRp activity of NS5B. In order to examine whether the HCV NS3 could affect RNA synthesis by the HCV RNA polymerase in vitro, we used two previously characterized RNA templates that are both capable of directing de novo initiation (Fig. 9A) (45, 46). A short 21-nt RNA named LE21 can form a quasi-stable intramolecular hairpin with a single-stranded 3′ sequence that is capable of directing de novo initiation of RNA synthesis. When the polymerase reaches the

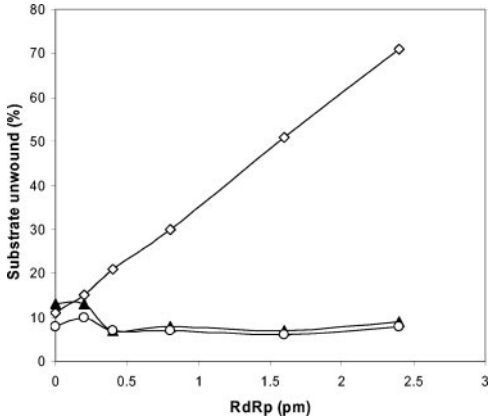

FIG. 6. Specificity of NS3 helicase stimulation by HCV RdRp. A viral RdRp derived from WNV was used as a nonspecific control to compare with HCV RdRp in stimulation of the NS3FL helicase. The dsDNA substrate was incubated with 0.1 pmol NS3FL or 0.5 pmol NS3H and increasing amounts of either HCV NS5B or WNV NS5 at 37°C for 30 min. A 0.5-pmol aliquot of NS3H was used here, which achieved an unwinding efficiency approximately equivalent to 0.1 pmol NS3FL, since the helicase activity of NS3H is about fivefold lower than that of NS3FL. The unwound products were separated by electrophoresis in a 12% native polyacrylamide gel, visualized by autoradiograph, and quantified with a phosphorimager. ◇, 0.1 pmol NS3FL plus NS5B; ▲, 0.5 pmol NS3H plus NS5B; ○, 0.1 pmol NS3FL plus WNV NS5.

Downloaded from http://jvi.asm.org/ on September 12, 2018 by guest

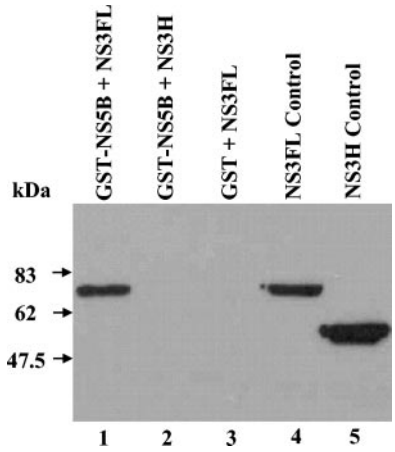

FIG. 7. Determination of NS3FL-NS5B interaction by GST pull-down. A GST-NS5B fusion protein or GST alone (as a control) was first incubated with glutathione-agarose gel. After washing, the GST or GST-NS5B-bound gel was subsequently incubated with NS3FL or NS3H, respectively. The NS3 proteins pulled down by NS5B were then determined by Western blot analysis using a monoclonal anti-NS3H antibody. Purified recombinant NS3FL and NS3H were used as positive controls for Western blot analysis. The sizes of protein molecular mass markers are indicated on the left.

5′ end of LE21, it could either terminate RNA synthesis, thus producing a 21-nt de novo-initiated RNA, or use a second template to generate a recombinant RNA product of 42 nt. In addition, two molecules of LE21 can partially anneal to direct primer-dependent RNA synthesis, generating a 34-nt product. The addition of either NS3H or NS3FL did not significantly alter the type or the amount of products synthesized by NS5BΔ21. To ensure that the lack of the C-terminal 21 amino acids did not prevent a possible effect of NS3, we also tested a full-length NS5B protein. Again, no significant effect on RNA synthesis was observed in the presence of NS3H or NS3FL. In some experiments, we did observe a 20 to 30% decrease in the amount of products made from LE21 in the presence of NS3FL (R. Kumar, unpublished data).

The lack of an effect on RNA synthesis from LE21 could be because it lacks a sufficiently structured region that would require the function of an RNA helicase. To examine this possibility, we used the 121-nt RNA derived from the 3′ end of the HCV minus-strand RNA genomes as a template. Unexpectedly, we found that the addition of NS3FL or NS3H at higher concentrations inhibited RNA synthesis by NS5BΔ21 in our standard reaction. One possible reason for this is that the ATPase activity of NS3 could decrease the concentration of the already low concentration of radiolabeled nucleotide (0.3 μM final concentration) and that the longer length of H121 exacerbated the inhibitory effect in comparison to product synthesis from LE21. We have also tested RNA syntheses using [α-^{32}P]CTP and [α-^{32}P]UTP as radiolabels and observed that NS3H or NS3FL also inhibited RNA synthesis from H121. One alternative interpretation for the inhibition of RNA synthesis is that the NS3 competes with NS5B for RNA template, since NS3 possesses an RNA-binding activity.

DISCUSSION

A consensus has not been reached as to whether the two distinctive NS3 enzymes are functionally interdependent between the protease and helicase domains. A number of studies have demonstrated that both the full-length NS3 and the truncated protease domain alone have comparable protease activities in vitro, suggesting that the NS3 protease does not depend on the presence of the NS3 helicase domain (14, 15, 22, 50, 55). We have evidence from this study to show that both NS3FL and NS3H have comparable NTPase activities. Therefore, some activities of NS3 can be functionally independent. However, contradicting evidence exists to either support or oppose a role of the NS3 protease domain in the modulation of its helicase activity (14, 15, 23, 40, 42). Several studies have revealed that the NS3 helicase activity is significantly enhanced

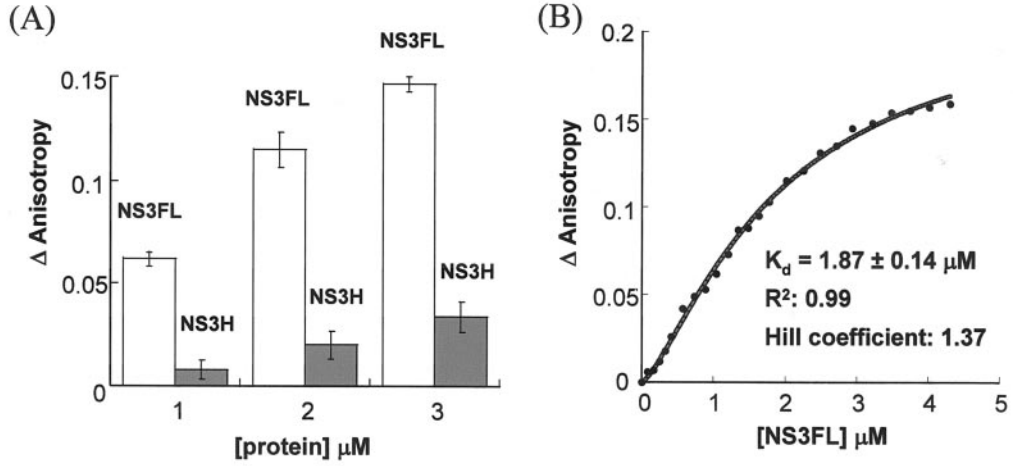

FIG. 8. Analysis of NS5B-NS3 interaction using fluorescence anisotropy. (A) A comparison of the interaction of between fluorescent-labeled NS5B and either NS3H or NS3FL. Each change in anisotropy value represents the mean and one deviation from 10 measurements. (B) Fluorescence anisotropy experiment to determine the affinity of the NS5B-NS3FL interaction. NS5B bound to the fluorescent dye FlAsH was determined in the presence of increasing concentrations of NS3FL. Each data point represents the average of 10 independent measurements. The K_d for the interaction was derived from the binding isotherm using the Hill equation, as described in Materials and Methods.

Downloaded from http://jvi.asm.org/ on September 12, 2018 by guest

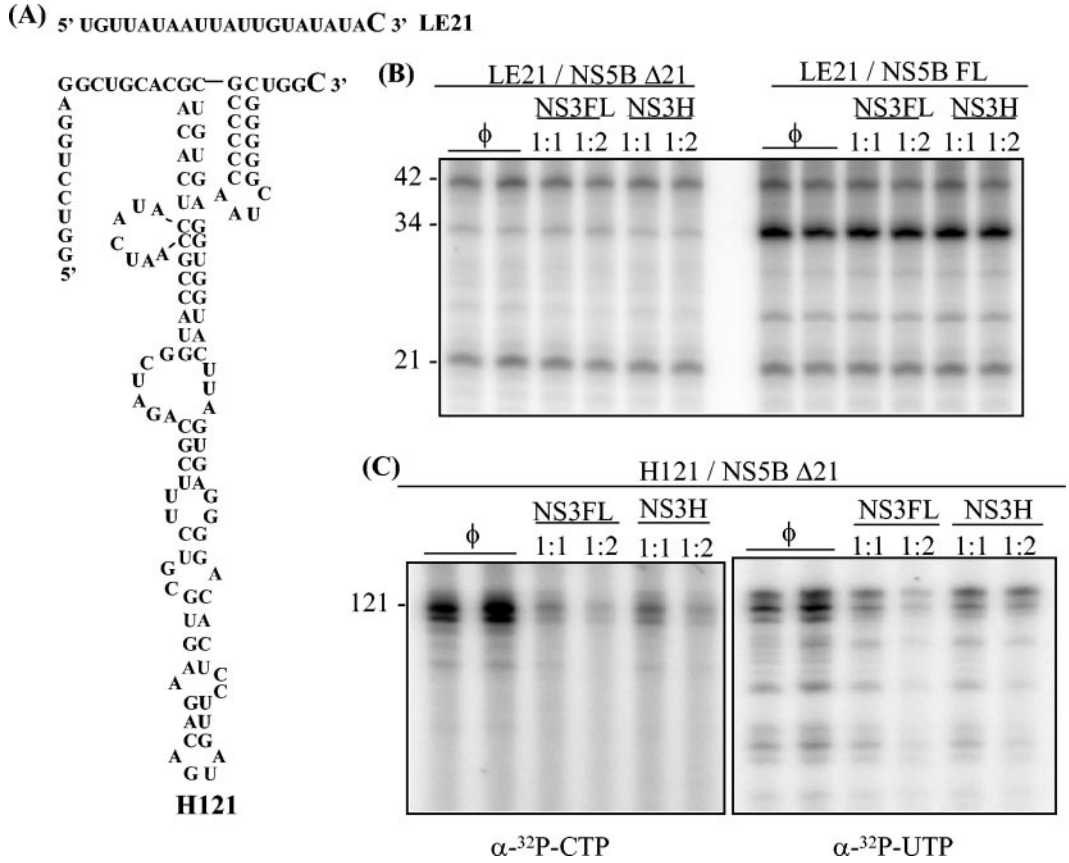

FIG. 9. Examination of the effects of NS3H or NS3-FL on polymerase activity of NS5B. (A) RNA templates used in the NS5B polymerase assay. LE21 was previously characterized by Ranjith-Kumar et al. (45). H121 was derived from the 3′-terminal 121 nt of the HCV minus-strand RNA, and its ability to direct RNA synthesis was characterized by Ranjith-Kumar et al. (46). (B) Gel image of RNAs synthesized by either NS5BΔ21 or full-length NS5B in the absence of NS3 (denoted with ϕ). The identities of the proteins added to the reaction mixtures are indicated above the lanes, and the ratios indicate the stoichiometric amounts of NS5B and the appropriate NS3 protein. The sizes of the RNA products are indicated to the right of the gel image. The 21-nt RNA was initiated de novo, the 34-nt RNA is the product of primer extension, and the 42-nt RNA is the result of RNA synthesis from two noncovalently linked templates (45). (C) RNA synthesis by HCV NS5BΔ21 using H121 as template. The identities of the proteins added to the reaction mixtures and their ratios relative to NS5BΔ21 are shown above the lanes in the gel. Because NS3 could hydrolyze purine triphosphates, [α-^{32}P]CTP and [α-^{32}P]UTP were used as the radiolabeled nucleotides in the reactions shown in the gel images to the right and left, respectively.

by the presence of the NS3 protease domain, as determined by a direct comparison of the helicase activities between NS3FL and NS3H (23, 40, 42). Consistent with this finding, NS4A was found to further increase the helicase activity of NS3FL by forming a noncovalent complex with the protease (23). However, these findings were not reproduced by other studies, which did not reveal a significant difference in the helicase/NTPase activities between full-length NS3 and the C-terminal helicase domain (14, 15). Conversely, NS4A was reported to inhibit rather than promote the NS3 helicase activity (15). In contrast, findings from our studies herein clearly demonstrate that the presence of the NS3 protease domain substantially increased the NS3 helicase activity. At least fivefold higher helicase activity was observed for the NS3FL than NS3H (Fig. 3). The lower helicase activity associated with the NS3H could not be explained by any significant difference in protein folding of the helicase in the absence of the protease domain. Previous crystallographic studies have determined that the X-ray structure of the helicase domain itself is similar to the one found in the full-length NS3 (6, 27, 61, 62), suggesting that the helicase domain itself, when expressed separately, was properly folded. Further support to this interpretation comes from the findings that the NTPase activity of the helicase domain (NS3H) was linearly correlated with enzyme concentrations and was comparable to that of the NS3FL (Fig. 3), indicating that the helicase was correctly folded. Furthermore, the helicase activity of NS3FL was enhanced by the addition of an increasing concentration of a synthetic NS4A core peptide (data not shown). Taken together, these findings demonstrate that the NS3 protease domain does up-regulate the NS3 helicase activity. This conclusion is supported by findings derived from several other studies (22, 23, 40, 42). However, Gallinari et al. did not observe a significant difference in helicase activity between NS3FL and NS3H (14, 15). The reason for the discrepancy between our results and those of Gallinari et al. is not clear (14, 15).

How the NS3 helicase activity is activated by the presence of its protease domain has not been fully illustrated. Although the NS3 helicase activity is coupled with its NTPase activity (30), our findings demonstrate that the enhancement of the NS3

Downloaded from http://jvi.asm.org/ on September 12, 2018 by guest

helicase by the protease domain was not due to activation of the NTPase activity. NS3FL was found to exhibit a substantially higher helicase activity than NS3H, but it did not affect the level of its NTPase activity (Fig. 3). These findings suggest that the protease domain can directly activate the helicase without an effect on the NTPase activity. Consistent with an earlier observation that NS4A was able to enhance functional NS3-RNA complex formation (42), an NS4A core peptide was also found to significantly enhance the NS3 helicase activity (data not shown). NS4A is known to bind tightly to the protease domain of NS3 and to stabilize the NS3 structure (28, 35, 60), which is required for protease activity. Likewise, stabilization of NS3 by NS4A may also convert NS3 into a more active helicase. The molecular basis underlying the helicase enhancement by the protease domain is probably best explained by the atomic structure of the full-length NS3 (62). The protease and helicase domains are segregated and covalently connected by a short strand. A number of amino acid residues of each domain are involved in the surface interaction at the domain interface. Additionally, there are extensive hydrogen bond interactions between the region containing the protease active site and the C-terminal six residues of the helicase domain (62). These interactions probably stabilize the enzyme in a conformation optimal for helicase activity. Furthermore, the nucleic acid-binding sites on the protease surface may also contribute to the enhancement of the helicase activity by binding to the helicase substrate (62). Mutagenesis analysis to alter interactions between the NS3 protease and helicase domains will likely provide insights into the understanding of the structural basis for the functional dependence of the NS3 helicase on the protease domain.

In addition to the NS3 protease, HCV RdRp (NS5B) was found to strikingly stimulate the NS3 helicase activity by a specific protein-protein interaction with the NS3 protease domain (Fig. 7 and 8). This novel finding is strongly supported by several lines of evidence described in this report. First, NS5B stimulation of NS3FL helicase activity occurs in a dose-dependent manner (Fig. 5 and 6). In contrast, a nonspecific control RdRp derived from WNV had no effect on the HCV NS3 helicase activity (Fig. 6). Additionally, stimulation of the NS3 helicase by NS5B is strictly dependent on the presence of the protease domain, since NS5B failed to stimulate the helicase activity of the NS3H that did not contain the protease domain (Fig. 6). Similar to the NS3 protease domain, NS5B did not affect the NTPase activity of NS3FL (data not shown). Furthermore, it appeared that NS5B could inhibit the NS3 protease activity when an in vitro-translated NS5A-NS5B substrate was used in a protease assay (Z. Cai et al., unpublished result). These findings suggest that the protease domain is required for mediating the NS3-NS5B interaction. Such a protein-protein interaction was indeed confirmed by both GST pull-down assay and fluorescence spectroscopy analysis. NS5B was able to specifically pull down NS3FL but not the NS3H protein (Fig. 7). Likewise, fluorescence anisotropy analysis demonstrated that NS5B tightly interacted with NS3FL but not NS3H (Fig. 8). A specific interaction between NS5B and the NS3 protease domain appears to be a prerequisite for NS3 helicase stimulation by HCV RdRp. It is noteworthy that our results are contrary to a previous finding that NS5B could interact with the NS3 helicase domain alone, as shown by a membrane-binding assay (44). One possible explanation is that the difference may be attributed to a difference in the affinity of the NS5B interaction between NS3H and NS3FL.

It is not clear yet how NS5B interacts with the NS3 protease domain and how such an interaction subsequently activates the NS3 helicase activity. Understanding of these fundamental questions will inevitably help to illustrate the molecular mechanism of HCV RNA replication. As discussed above, the C terminus of NS3 forms hydrogen bond interactions with the protease domain near the enzyme active site after *cis*-cleavage by the NS3 protease (62). The N-terminal portion of NS5B may interact with the protease domain through the protease active site in a manner similar to the C-terminal portion of NS3, as revealed by the structure of a single-chain NS3-NS4A molecule (62). The NS5B N terminus is the P′-side product of the cleavage by the NS3 serine protease at the NS5A and NS5B junction. There could be other regions involved in the interaction between these two molecules. Upon interaction with the protease domain, NS5B may cause a conformational rearrangement of the NS3 helicase, which could increase substrate unwinding.

Replication of most positive-strand RNA viruses takes place in the membrane-bound replication complex consisting of viral RNA, most NS proteins, and cellular proteins as well. The viral replicase proteins were found to interact with each other in the intracellular sites where viral RNA is replicated (11, 12, 41, 54). Therefore, it is conceivable that the replicase proteins affect/regulate each other's properties through protein-protein interactions. The HCV NS3 represents the first viral RNA helicase whose function is stimulated by a viral RNA polymerase. Our findings also provide an explanation for the existence of two apparently functionally independent distinct activities (protease and helicase/NTPase) within one NS3 molecule. The NS3 protease domain functions not only as an enzyme but also as a mediator for a specific interaction with NS5B, which enhances the NS3 helicase activity.

As to the role of NS3 in RNA synthesis in vitro, our results contrast with those previously reported by Piccininni et al., who observed an unexpected multimeric product made from the input template in the presence of NS3FL (44). This difference is especially notable because both studies used a template derived from the 3′ end of minus-strand HCV RNA. We speculate that the difference is due to the ratio of NS5B to template used in our respective reaction mixtures. Piccininni et al. used 6.4-fold more enzyme than template RNA, while our reaction mixtures had an equal or higher molar ratio of enzyme to template. The multimeric product in the presence of NS3, observed in the study by Piccininni et al., is inconsistent with de novo RNA synthesis during HCV RNA replication. The primary mode of RNA synthesis during HCV replication in vivo is initiated by a de novo mechanism. Despite the differences, neither study observed that NS3FL or NS3H could increase de novo RNA synthesis (Fig. 9) (43). In fact, both studies showed that in the presence of 0.5 mM ATP or below, NS3 actually decreased RNA synthesis by NS5B, possibly due to the NTPase activity of NS3 decreasing the NTP concentration needed for efficient RNA synthesis or the RNA-binding activity of NS3 that competes for the RNA template with NS5B.

In summary, the NS3 helicase activity is differentially modulated by the presence of the NS3 protease domain as well as

Downloaded from http://jvi.asm.org/ on September 12, 2018 by guest

the viral RNA polymerase. Perhaps NS3 initially functions as a protease responsible for viral polyprotein processing. Once recruited into the HCV replication complex containing NS5B, NS3 switches to serving as the helicase/NTPase that is required for HCV RNA replication.

ACKNOWLEDGMENTS

We thank Jackie Wright-Minogue at Schering-Plough Research Institute for kindly providing us with synthetic NS4A core peptides and Kyung-Soo Chang for the NS3H and NS5B monoclonal antibodies.

This work was supported by a grant from the National Institutes of Health (CA093712 to G.L.) and in part by a grant from the Kentucky Science and Engineering Foundation (KSEF-148-502-02-18 to G.L.). C.K. acknowledges funding from National Science Foundation grant MCB0332259. P.-Y.S. was in part supported by a developmental project from Northeast Biodefense Center.

Chen Zhang and Zhaohui Cai contributed equally to this work.

REFERENCES

1. **Bartenschlager, R., L. Ahlborn-Laake, J. Mous, and H. Jacobsen.** 1993. Nonstructural protein 3 of the hepatitis C virus encodes a serine-type proteinase required for cleavage at the NS3/4 and NS4/5 junctions. J. Virol. **67:**3835–3844.
2. **Bartosch, B., J. Dubuisson, and F. L. Cosset.** 2003. Infectious hepatitis C virus pseudo-particles containing functional E1-E2 envelope protein complexes. J. Exp. Med. **197:**633–642.
3. **Baumert, T. F., S. Ito, D. T. Wong, and T. J. Liang.** 1998. Hepatitis C virus structural proteins assemble into virus-like particles in insect cells. J. Virol. **72:**3827–3836.
4. **Behrens, S. E., L. Tomei, and R. De Francesco.** 1996. Identification and properties of the RNA-dependent RNA polymerase of hepatitis C virus. EMBO J. **15:**12–22.
5. **Blight, K. J., A. A. Kolykhalov, and C. M. Rice.** 2000. Efficient initiation of HCV RNA replication in cell culture. Science **290:**1972–1975.
6. **Cho, H. S., N. C. Ha, L. W. Kang, K. M. Chung, S. H. Back, S. K. Jang, and B. H. Oh.** 1998. Crystal structure of RNA helicase from genotype 1b hepatitis C virus. A feasible mechanism of unwinding duplex RNA. J. Biol. Chem. **273:**15045–15052.
7. **Choo, Q. L., G. Kuo, A. J. Weiner, L. R. Overby, D. W. Bradley, and M. Houghton.** 1989. Isolation of a cDNA clone derived from a blood-borne non-A, non-B viral hepatitis genome. Science **244:**359–362.
8. **Choo, Q. L., K. H. Richman, J. H. Han, K. Berger, C. Lee, C. Dong, C. Gallegos, D. Coit, R. Medina-Selby, P. J. Barr, et al.** 1991. Genetic organization and diversity of the hepatitis C virus. Proc. Natl. Acad. Sci. USA **88:**2451–2455.
9. **Cui, T., R. J. Sugrue, Q. Xu, A. K. Lee, Y. C. Chan, and J. Fu.** 1998. Recombinant dengue virus type 1 NS3 protein exhibits specific viral RNA binding and NTPase activity regulated by the NS5 protein. Virology **246:** 409–417.
10. **De Francesco, R., and C. Steinkuhler.** 2000. Structure and function of the hepatitis C virus NS3-NS4A serine proteinase. Curr. Top. Microbiol. Immunol. **242:**149–169.
11. **Egger, D., B. Wolk, R. Gosert, L. Bianchi, H. E. Blum, D. Moradpour, and K. Bienz.** 2002. Expression of hepatitis C virus proteins induces distinct membrane alterations including a candidate viral replication complex. J. Virol. **76:**5974–5984.
12. **El-Hage, N., and G. Luo.** 2003. Replication of hepatitis C virus RNA occurs in a membrane-bound replication complex containing nonstructural viral proteins and RNA. J. Gen. Virol. **84:**2761–2769.
13. **Forns, X., R. Thimme, S. Govindarajan, S. U. Emerson, R. H. Purcell, F. V. Chisari, and J. Bukh.** 2000. Hepatitis C virus lacking the hypervariable region 1 of the second envelope protein is infectious and causes acute resolving or persistent infection in chimpanzees. Proc. Natl. Acad. Sci. USA **97:**13318–13323.
14. **Gallinari, P., D. Brennan, C. Nardi, M. Brunetti, L. Tomei, C. Steinkuhler, and R. De Francesco.** 1998. Multiple enzymatic activities associated with recombinant NS3 protein of hepatitis C virus. J. Virol. **72:**6758–6769.
15. **Gallinari, P., C. Paolini, D. Brennan, C. Nardi, C. Steinkuhler, and R. De Francesco.** 1999. Modulation of hepatitis C virus NS3 protease and helicase activities through the interaction with NS4A. Biochemistry **38:**5620–5632.
16. **Grakoui, A., D. W. McCourt, C. Wychowski, S. M. Feinstone, and C. M. Rice.** 1993. A second hepatitis C virus-encoded proteinase. Proc. Natl. Acad. Sci. USA **90:**10583–10587.
17. **Grakoui, A., C. Wychowski, C. Lin, S. M. Feinstone, and C. M. Rice.** 1993. Expression and identification of hepatitis C virus polyprotein cleavage products. J. Virol. **67:**1385–1395.
18. **Griffin, B. A., S. R. Adams, J. Jones, and R. Y. Tsien.** 2000. Fluorescent labeling of recombinant proteins in living cells with FlAsH. Methods Enzymol. **327:**565–578.
19. **Gwack, Y., D. W. Kim, J. H. Han, and J. Choe.** 1996. Characterization of RNA binding activity and RNA helicase activity of the hepatitis C virus NS3 protein. Biochem. Biophys. Res. Commun. **225:**654–659.
20. **Gwack, Y., D. W. Kim, J. H. Han, and J. Choe.** 1997. DNA helicase activity of the hepatitis C virus nonstructural protein 3. Eur. J. Biochem. **250:**47–54.
21. **Hijikata, M., H. Mizushima, T. Akagi, S. Mori, N. Kakiuchi, N. Kato, T. Tanaka, K. Kimura, and K. Shimotohno.** 1993. Two distinct proteinase activities required for the processing of a putative nonstructural precursor protein of hepatitis C virus. J. Virol. **67:**4665–4675.
22. **Hong, Z., E. Ferrari, J. Wright-Minogue, R. Chase, C. Risano, G. Seelig, C. G. Lee, and A. D. Kwong.** 1996. Enzymatic characterization of hepatitis C virus NS3/4A complexes expressed in mammalian cells by using the herpes simplex virus amplicon system. J. Virol. **70:**4261–4268.
23. **Howe, A. Y., R. Chase, S. S. Taremi, C. Risano, B. Beyer, B. Malcolm, and J. Y. Lau.** 1999. A novel recombinant single-chain hepatitis C virus NS3-NS4A protein with improved helicase activity. Protein Sci. **8:**1332–1341.
24. **Ishido, S., T. Fujita, and H. Hotta.** 1998. Complex formation of NS5B with NS3 and NS4A proteins of hepatitis C virus. Biochem. Biophys. Res. Commun. **244:**35–40.
25. **Jin, L., and D. L. Peterson.** 1995. Expression, isolation, and characterization of the hepatitis C virus ATPase/RNA helicase. Arch. Biochem. Biophys. **323:**47–53.
26. **Kim, D. W., Y. Gwack, J. H. Han, and J. Choe.** 1995. C-terminal domain of the hepatitis C virus NS3 protein contains an RNA helicase activity. Biochem. Biophys. Res. Commun. **215:**160–166.
27. **Kim, J. L., K. A. Morgenstern, J. P. Griffith, M. D. Dwyer, J. A. Thomson, M. A. Murcko, C. Lin, and P. R. Caron.** 1998. Hepatitis C virus NS3 RNA helicase domain with a bound oligonucleotide: the crystal structure provides insights into the mode of unwinding. Structure **6:**89–100.
28. **Kim, J. L., K. A. Morgenstern, C. Lin, T. Fox, M. D. Dwyer, J. A. Landro, S. P. Chambers, W. Markland, C. A. Lepre, E. T. O'Malley, S. L. Harbeson, C. M. Rice, M. A. Murcko, P. R. Caron, and J. A. Thomson.** 1996. Crystal structure of the hepatitis C virus NS3 protease domain complexed with a synthetic NS4A cofactor peptide. Cell **87:**343–355. [Erratum, **89:**159, 1997.]
29. **Kolykhalov, A. A., K. Mihalik, S. M. Feinstone, and C. M. Rice.** 2000. Hepatitis C virus-encoded enzymatic activities and conserved RNA elements in the 3′ nontranslated region are essential for virus replication in vivo. J. Virol. **74:**2046–2051.
30. **Kwong, A. D., J. L. Kim, and C. Lin.** 2000. Structure and function of hepatitis C virus NS3 helicase. Curr. Top. Microbiol. Immunol. **242:**171–196.
31. **Lin, C., B. D. Lindenbach, B. M. Pragai, D. W. McCourt, and C. M. Rice.** 1994. Processing in the hepatitis C virus E2-NS2 region: identification of p7 and two distinct E2-specific products with different C termini. J. Virol. **68:**5063–5073.
32. **Lin, C., B. M. Pragai, A. Grakoui, J. Xu, and C. M. Rice.** 1994. Hepatitis C virus NS3 serine proteinase: trans-cleavage requirements and processing kinetics. J. Virol. **68:**8147–8157.
33. **Lin, C., and C. M. Rice.** 1995. The hepatitis C virus NS3 serine proteinase and NS4A cofactor: establishment of a cell-free trans-processing assay. Proc. Natl. Acad. Sci. USA **92:**7622–7626.
34. **Lohmann, V., F. Korner, J. Koch, U. Herian, L. Theilmann, and R. Bartenschlager.** 1999. Replication of subgenomic hepatitis C virus RNAs in a hepatoma cell line. Science **285:**110–113.
35. **Love, R. A., H. E. Parge, J. A. Wickersham, Z. Hostomsky, N. Habuka, E. W. Moomaw, T. Adachi, and Z. Hostomska.** 1996. The crystal structure of hepatitis C virus NS3 proteinase reveals a trypsin-like fold and a structural zinc binding site. Cell **87:**331–342.
36. **Luo, G.** 2004. Molecular virology of hepatitis C virus. Birkhauser, Basel, Switzerland.
37. **Luo, G., S. Xin, and Z. Cai.** 2003. Role of the 5′-proximal stem-loop structure of the 5′ untranslated region in replication and translation of hepatitis C virus RNA. J. Virol. **77:**3312–3318.
38. **Markland, W., R. A. Petrillo, M. Fitzgibbon, T. Fox, R. McCarrick, T. McQuaid, J. R. Fulghum, W. Chen, M. A. Fleming, J. A. Thomson, and S. P. Chambers.** 1997. Purification and characterization of the NS3 serine protease domain of hepatitis C virus expressed in Saccharomyces cerevisiae. J. Gen. Virol. **78:**39–43.
39. **McKeating, J. A., L. Q. Zhang, C. Logvinoff, M. Flint, J. Zhang, J. Yu, D. Butera, D. D. Ho, L. B. Dustin, C. M. Rice, and P. Balfe.** 2004. Diverse hepatitis C virus glycoproteins mediate viral infection in a CD81-dependent manner. J. Virol. **78:**8496–8505.
40. **Morgenstern, K. A., J. A. Landro, K. Hsiao, C. Lin, Y. Gu, M. S. Su, and J. A. Thomson.** 1997. Polynucleotide modulation of the protease, nucleoside triphosphatase, and helicase activities of a hepatitis C virus NS3-NS4A complex isolated from transfected COS cells. J. Virol. **71:**3767–3775.
41. **Mottola, G., G. Cardinali, A. Ceccacci, C. Trozzi, L. Bartholomew, M. R. Torrisi, E. Pedrazzini, S. Bonatti, and G. Migliaccio.** 2002. Hepatitis C virus nonstructural proteins are localized in a modified endoplasmic reticulum of cells expressing viral subgenomic replicons. Virology **293:**31–43.
42. **Pang, P. S., E. Jankowsky, P. J. Planet, and A. M. Pyle.** 2002. The hepatitis

Downloaded from http://jvi.asm.org/ on September 12, 2018 by guest

C viral NS3 protein is a processive DNA helicase with cofactor enhanced RNA unwinding. EMBO J. **21:**1168–1176.
43. **Paolini, C., R. De Francesco, and P. Gallinari.** 2000. Enzymatic properties of hepatitis C virus NS3-associated helicase. J. Gen. Virol. **81:**1335–1345.
44. **Piccininni, S., A. Varaklioti, M. Nardelli, B. Dave, K. D. Raney, and J. E. McCarthy.** 2002. Modulation of the hepatitis C virus RNA-dependent RNA polymerase activity by the non-structural (NS) 3 helicase and the NS4B membrane protein. J. Biol. Chem. **277:**45670–45679.
45. **Ranjith-Kumar, C. T., Y. C. Kim, L. Gutshall, C. Silverman, S. Khandekar, R. T. Sarisky, and C. C. Kao.** 2002. Mechanism of de novo initiation by the hepatitis C virus RNA-dependent RNA polymerase: role of divalent metals. J. Virol. **76:**12513–12525.
46. **Ranjith-Kumar, C. T., J. L. Santos, L. L. Gutshall, V. K. Johnston, J. Lin-Goerke, M. J. Kim, D. J. Porter, D. Maley, C. Greenwood, D. L. Earnshaw, A. Baker, B. Gu, C. Silverman, R. T. Sarisky, and C. Kao.** 2003. Enzymatic activities of the GB virus-B RNA-dependent RNA polymerase. Virology **312:**270–280.
47. **Reed, K. E., and C. M. Rice.** 2000. Overview of hepatitis C virus genome structure, polyprotein processing, and protein properties. Curr. Top. Microbiol. Immunol. **242:**55–84.
48. **Robertson, B., G. Myers, C. Howard, T. Brettin, J. Bukh, B. Gaschen, T. Gojobori, G. Maertens, M. Mizokami, O. Nainan, S. Netesov, K. Nishioka, T. Shin i, P. Simmonds, D. Smith, L. Stuyver, A. Weiner, et al.** 1998. Classification, nomenclature, and database development for hepatitis C virus (HCV) and related viruses: proposals for standardization. Arch. Virol. **143:** 2493–2503.
49. **Sakai, A., M. S. Claire, K. Faulk, S. Govindarajan, S. U. Emerson, R. H. Purcell, and J. Bukh.** 2003. The p7 polypeptide of hepatitis C virus is critical for infectivity and contains functionally important genotype-specific sequences. Proc. Natl. Acad. Sci. USA **100:**11646–11651.
50. **Sali, D. L., R. Ingram, M. Wendel, D. Gupta, C. McNemar, A. Tsarbopoulos, J. W. Chen, Z. Hong, R. Chase, C. Risano, R. Zhang, N. Yao, A. D. Kwong, L. Ramanathan, H. V. Le, and P. C. Weber.** 1998. Serine protease of hepatitis C virus expressed in insect cells as the NS3/4A complex. Biochemistry **37:** 3392–3401.
51. **Seeff, L. B., and J. H. Hoofnagle.** 2002. National Institutes of Health Consensus Development Conference: management of hepatitis C, 2002. Hepatology **36:**S1–S2.
52. **Selby, M. J., Q. L. Choo, K. Berger, G. Kuo, E. Glazer, M. Eckart, C. Lee, D. Chien, C. Kuo, and M. Houghton.** 1993. Expression, identification and subcellular localization of the proteins encoded by the hepatitis C viral genome. J. Gen. Virol. **74:**1103–1113.
53. **Shi, P. Y., M. Tilgner, M. K. Lo, K. A. Kent, and K. A. Bernard.** 2002. Infectious cDNA clone of the epidemic West Nile virus from New York City. J. Virol. **76:**5847–5856.
54. **Shi, S. T., K. J. Lee, H. Aizaki, S. B. Hwang, and M. M. Lai.** 2003. Hepatitis C virus RNA replication occurs on a detergent-resistant membrane that cofractionates with caveolin-2. J. Virol. **77:**4160–4168.
55. **Steinkuhler, C., L. Tomei, and R. De Francesco.** 1996. In vitro activity of hepatitis C virus protease NS3 purified from recombinant baculovirus-infected Sf9 cells. J. Biol. Chem. **271:**6367–6373.
56. **Suzich, J. A., J. K. Tamura, F. Palmer-Hill, P. Warrener, A. Grakoui, C. M. Rice, S. M. Feinstone, and M. S. Collett.** 1993. Hepatitis C virus NS3 protein polynucleotide-stimulated nucleoside triphosphatase and comparison with the related pestivirus and flavivirus enzymes. J. Virol. **67:**6152–6158.
57. **World Health Organization.** 1998. W.H.O. concerns: hepatitis C. Lancet **351:**1415.
58. **Wright-Minogue, J., N. Yao, R. Zhang, N. J. Butkiewicz, B. M. Baroudy, J. Y. Lau, and Z. Hong.** 2000. Cross-genotypic interaction between hepatitis C virus NS3 protease domains and NS4A cofactors. J. Hepatol. **32:**497–504.
59. **Wu, Z., N. Yao, H. V. Le, and P. C. Weber.** 1998. Mechanism of autoproteolysis at the NS2-NS3 junction of the hepatitis C virus polyprotein. Trends Biochem. Sci. **23:**92–94.
60. **Yan, Y., Y. Li, S. Munshi, V. Sardana, J. L. Cole, M. Sardana, C. Steinkuehler, L. Tomei, R. De Francesco, L. C. Kuo, and Z. Chen.** 1998. Complex of NS3 protease and NS4A peptide of BK strain hepatitis C virus: a 2.2 Å resolution structure in a hexagonal crystal form. Protein Sci. **7:**837–847.
61. **Yao, N., T. Hesson, M. Cable, Z. Hong, A. D. Kwong, H. V. Le, and P. C. Weber.** 1997. Structure of the hepatitis C virus RNA helicase domain. Nat. Struct. Biol. **4:**463–467.
62. **Yao, N., P. Reichert, S. S. Taremi, W. W. Prosise, and P. C. Weber.** 1999. Molecular views of viral polyprotein processing revealed by the crystal structure of the hepatitis C virus bifunctional protease-helicase. Struct. Fold Des. **7:**1353–1363.

Downloaded from http://jvi.asm.org/ on September 12, 2018 by guest